



RESEARCH DEPARTMENT

REPORT

SURFACE-ACOUSTIC-WAVES: experimental device fabrication

A. Roberts, B.Eng.
K. Hacking, B.Sc.

SURFACE-ACOUSTIC-WAVES: EXPERIMENTAL DEVICE FABRICATION

A. Roberts, B.Eng.
K. Hacking, B.Sc.

Summary

An experimental Surface-Acoustic-Wave (SAW) device production technique has been developed, using a stepping camera and safe chemical processes. Devices can be made, operating in the frequency range from 15 to 100 MHz on a variety of piezo-electric substrates. Delays, frequency filters and resonators are the most common types of device, but convolvers, dispersive filters and many other types can be produced.

The camera has proved accurate and reliable; its operation is automatically controlled from a punched data tape. The chemical processes require a high standard of care and cleanliness to achieve consistent results, but are capable of producing working devices up to 100 MHz. The stepping camera and the chemical processes are described, together with a brief introduction to the subject of Surface-Acoustic-Waves.

Issued under the authority of



Research Department, Engineering Division,
BRITISH BROADCASTING CORPORATION

December 1979
(PH-216)

Head of Research Department



SURFACE-ACOUSTIC-WAVES: EXPERIMENTAL DEVICE FABRICATION

Section	Title	Page
Summary	Title Page
1. Introduction	1
1.1. Surface-Acoustic-Waves	1
1.2. Aims of this research	3
2. The stepping camera	3
2.1. Construction	5
2.1.1. Object slit and lamp-house assembly	5
2.1.2. Lens and shutter assembly	5
2.1.3. Slide carrier and stepping table	5
2.2. Control	5
2.2.1. Manual controls	5
2.2.2. Automatic controls	6
2.3. Performance	6
2.3.1. Mechanical movements	6
2.3.1.1. 'Y' motion	6
2.3.1.2. Shutter motion	8
2.3.1.3. 'X' motion	8
2.3.1.4. Vernier crystal motion	8
2.3.2. Calibration	8
2.3.2.1. Focus	8
2.3.2.2. Exposure	9
2.3.2.3. Line width	9
3. Fabrication processes	10
3.1. Methods	10
3.2. Mask fabrication	11
3.2.1. Slide preparation	11
3.2.2. Metal coating	11
3.2.3. Resist coating	11
3.2.4. Exposing the resist	12
3.2.5. Image development	12
3.2.6. Etching	12
3.3. Fabrication of a device from a mask	13
3.3.1. Substrate mounting	13
3.3.2. Cleaning	13
3.3.3. Metal coating	13
3.3.4. Resist coating	13
3.3.5. Exposure and development	13
3.3.6. Etching	13
3.3.7. Mounting the device	13

Section	Title	Page
4. Conclusions		13
5. References		14

SURFACE-ACOUSTIC-WAVES: EXPERIMENTAL DEVICE FABRICATION

A. Roberts, B.Eng.
K. Hacking, B.Sc.

1. Introduction

Surface-Acoustic-Wave (SAW) devices offer the circuit designer a large range of monolithic filter types, from simple band-pass delays to convolvers, oscillators, modulators, opto-electronic and dispersive devices. Military communications and surveillance equipment now depend heavily on SAW devices and research funded by Governments has brought about a rapid increase in knowledge of them.

Fabrication of SAW devices has made extensive use of equipment designed for the integrated circuit industry; highly accurate artwork is photographically reduced to make a mask from which the device can be made by projection or contact exposure. Such methods are capable of producing devices working at frequencies above 1 GHz.

This Report describes apparatus and processes that have been developed at low cost for the production of SAW devices operating at frequencies up to about 100 MHz. Before dealing with the apparatus, an introduction to SAW devices is given.

1.1. Surface-Acoustic-Waves

An illustration of a surface-acoustic, or Rayleigh,¹ wave generated and propagated on anisotropic material is shown in Fig. 1. It is an elastic wave launched through the piezo-electric

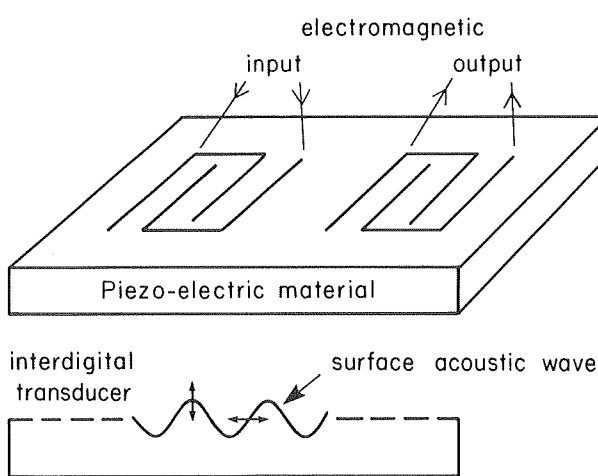


Fig. 1 - Representation of the launching and propagation of a Surface-Acoustic-Wave

effect by the field generated in the interdigital transducer² (IDT). The wave energy is normally confined to within a few wavelengths of the surface. The low surface-wave velocity, typically 10^{-5} of the electro-magnetic wave velocity, and the ease of electroacoustic coupling, suggest that SAW devices could conveniently provide highly compact transversal bandpass filters.

The surface wave is conventionally launched by an interdigital transducer, comprising two sets of interleaved metal strips, each set connected to the electrical circuit as shown in Fig. 2(a). Fig. 2(b) shows the locations of the unit impulses used to represent the transducer in the following analysis. An alternating voltage applied to the transducer produces an alternating electric field in and above the surface of the piezo-electric substrate. Through the piezo-electric effect, the surface is distorted in sympathy with the electric field and energy is transferred from the electrical input to the substrate. Constructive interference will occur at a frequency given by,

$$f_o = \frac{V}{d} \quad (1)$$

where V is the wave velocity, a constant for the material and propagation direction, and d is the transducer pitch (Fig. 2(a)).

The impulse response $b(t)$ of an IDT with $2A+1$ finger pairs is

$$b(t) = \sum_{n=-A}^{A} \delta(t - n\tau) \quad (2)$$

where $\tau = \frac{1}{f_o}$ is the period between delta functions.

The transfer function, or frequency response, $H(f)$, of the entire transducer is the Fourier transform of $b(t)$. For the case where the impulses are all of unit strength, $\delta(t) = +1$, it can be shown that,

$$H(f) = \frac{\sin(N\pi f/f_o)}{\sin(\pi f/f_o)} \quad (3)$$

where $N = 2A+1$, the number of finger pairs.

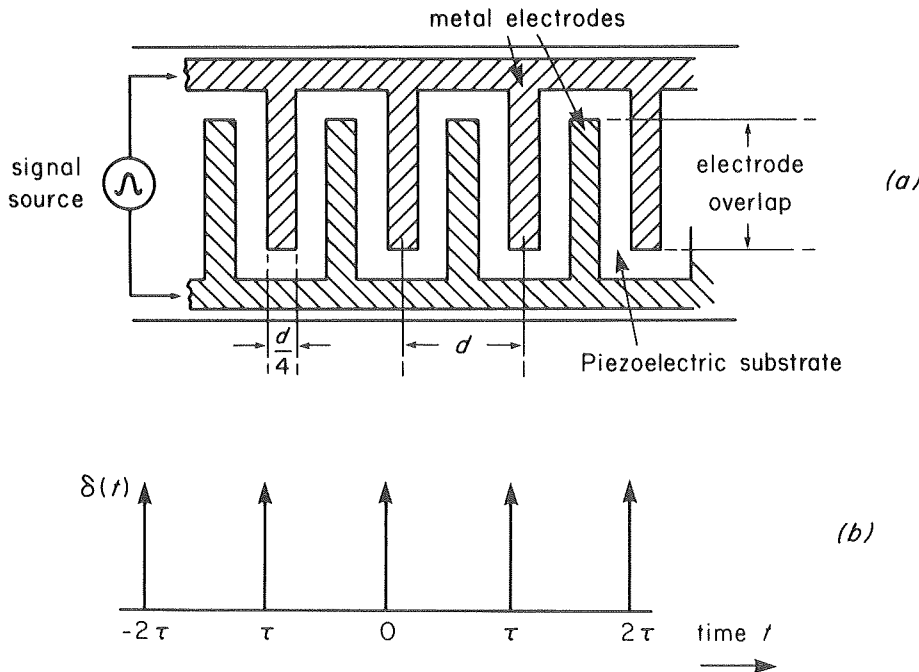


Fig. 2 - Unapodised interdigital transducer geometry

(a) Typical transducer pattern

(b) Representation of unit impulses used for transducer analysis

In the region of the frequency f_o (the 'centre frequency') and recognising that N is invariably much greater than unity, $H(f)$ can be written as

$$H(f) \simeq N \frac{\sin x}{x} \quad (4)$$

where

$$x = N\pi \left(\frac{f - f_o}{f_o} \right)$$

From this equation it is evident that $H(f)$ is zero (i.e. there is no surface wave) at frequencies given by $x = m\pi$, i.e. for

$$f = \frac{mf_o}{N} + f_o \quad (5)$$

where m is a non-zero integer.

Thus, the separation of the first zeros in the frequency response ($m = \pm 1$) is

$$f_1 = \frac{2f_o}{N} \quad (6)$$

The -3 dB bandwidth of such a transducer can be shown to be approximately f_o/N . It should be noted that this analysis applies equally to a

transducer producing an electrical output from an acoustic signal and that the transfer function of the entire device is the product of the transfer functions of the two transducers.

This simple transducer analysis can be used for the design of narrow bandwidth filters where N is large, but for asymmetric or wide-band filters a more complex approach is needed. This can most readily be done by varying the delta-function amplitudes within the transducer by apodisation; varying the overlap of the individual finger-pairs is a commonly used method of apodisation. Many other methods can be used, for example fingers can be selectively omitted or changed in phase. However, overlap weighting is a very convenient technique and has the advantage of representing graphically the impulse response of the transducer by the envelope of the finger ends.

The foregoing analysis assumes that the finger electrodes are massless and that the acoustic sources are mutually independent. In practice, however, even a thin aluminium electrode presents a small mass-loading of the surface which is sufficient to cause a partial reflection of acoustic waves from each finger edge. In a transducer of uniform pitch, these reflections add constructively at the centre frequency and generate a reflected wave which interferes with the wanted surface wave and upsets the characteristics of the device. One method frequently adopted to overcome this

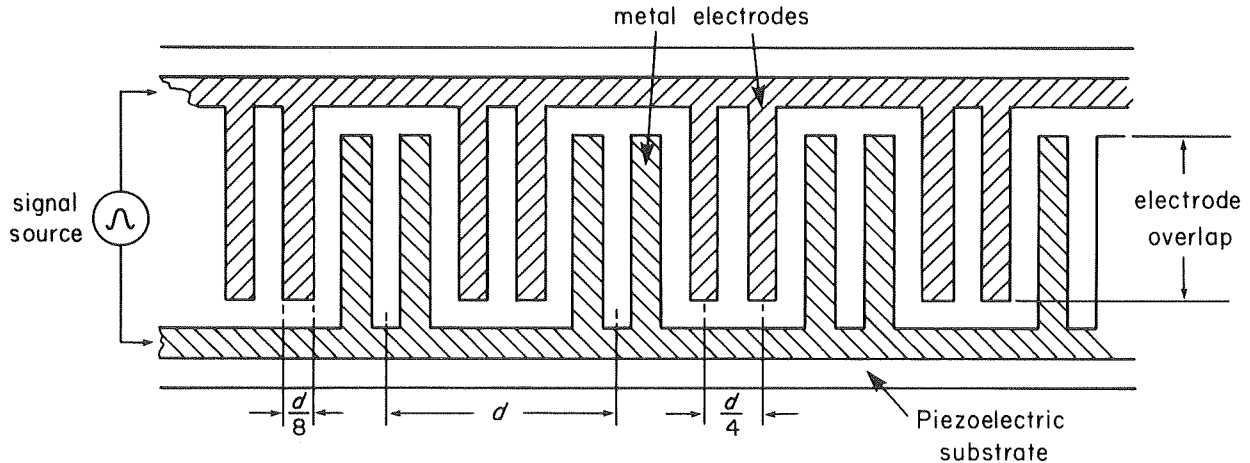


Fig. 3 - Transducer pattern with split-fingers

problem is to split each $d/4$ finger into two $d/8$ fingers with a $d/8$ gap between them, as shown in Fig. 3. Although there are now twice as many finger edges and, therefore, sources of reflected waves, at the centre frequency alternate reflected waves are in antiphase and so the overall result is suppression of reflected waves.

The materials most suited to SAW applications are piezo-electric, single crystals, sliced and oriented so that there is a strong coupling of energy into the surface-wave mode. Thus, in selecting a suitable material and orientation, the acousto-electric coupling coefficient, k , is an important feature. For most purposes, k^2 is used and can be defined, when k is small, by

$$k^2 = \frac{2\Delta V}{V} \quad (7)$$

where ΔV is the reduction in surface wave velocity caused by a massless metal (conductive) coating on the surface.

Slobodnik³ tabulates computed parameters of all the popular substrates, such as quartz and lithium niobate for most crystalline cuts and propagation directions. The reader is referred to some⁴⁻¹¹ of the abundance of literature on SAW devices for further information on properties, performance and types of devices.

1.2. Aims of this research

The purpose of this work was to establish a SAW device production facility, at low cost, avoiding the time-consuming artwork and photography stages common in commercial processes.¹² It was decided to construct a small stepping camera whereby masks could be produced directly;

the SAW device itself would be made by contact-printing from the mask. An arbitrary upper operating frequency of 100 MHz was specified although a limit of 50 MHz would be acceptable, the whole fabrication process was to be automated where possible, and ideally, take only 24 hours to specify and produce a device.

In some respects these aims have been met, in others they have not. An upper limit of 100 MHz applies to devices on substrates with low coupling coefficients such as quartz, but it is reduced to 50 MHz for low loss devices on highly efficient materials such as lithium niobate. Operation of the camera is mainly automatic, a device can be produced in 24 hours provided that all the equipment is in frequent use.

The types of device to be produced were not defined, but it was supposed that delays, frequency filters, resonators, dispersive (chirp) filters and oscillators could be made. At the time of writing, a small number of experimental devices have been made, delays and frequency filters, with highly encouraging results.

2. The stepping camera

The camera is shown in Fig. 4. It comprises a rear-illuminated object in the shape of a single slit, but with widened ends to form the bus-bar connections, a lens and shutter, and a slide holder mounted in a stepping-table; it was designed and made in the Model Shop.* Images of the slit are exposed, one at a time, on to a photo-sensitive slide in the holder, the 'X' stepping-table moving the plate by the required inter-electrode spacing. The image reduction is 9 : 1.

* This work was done mainly by D.H. Rumsey and C.W. Woods.

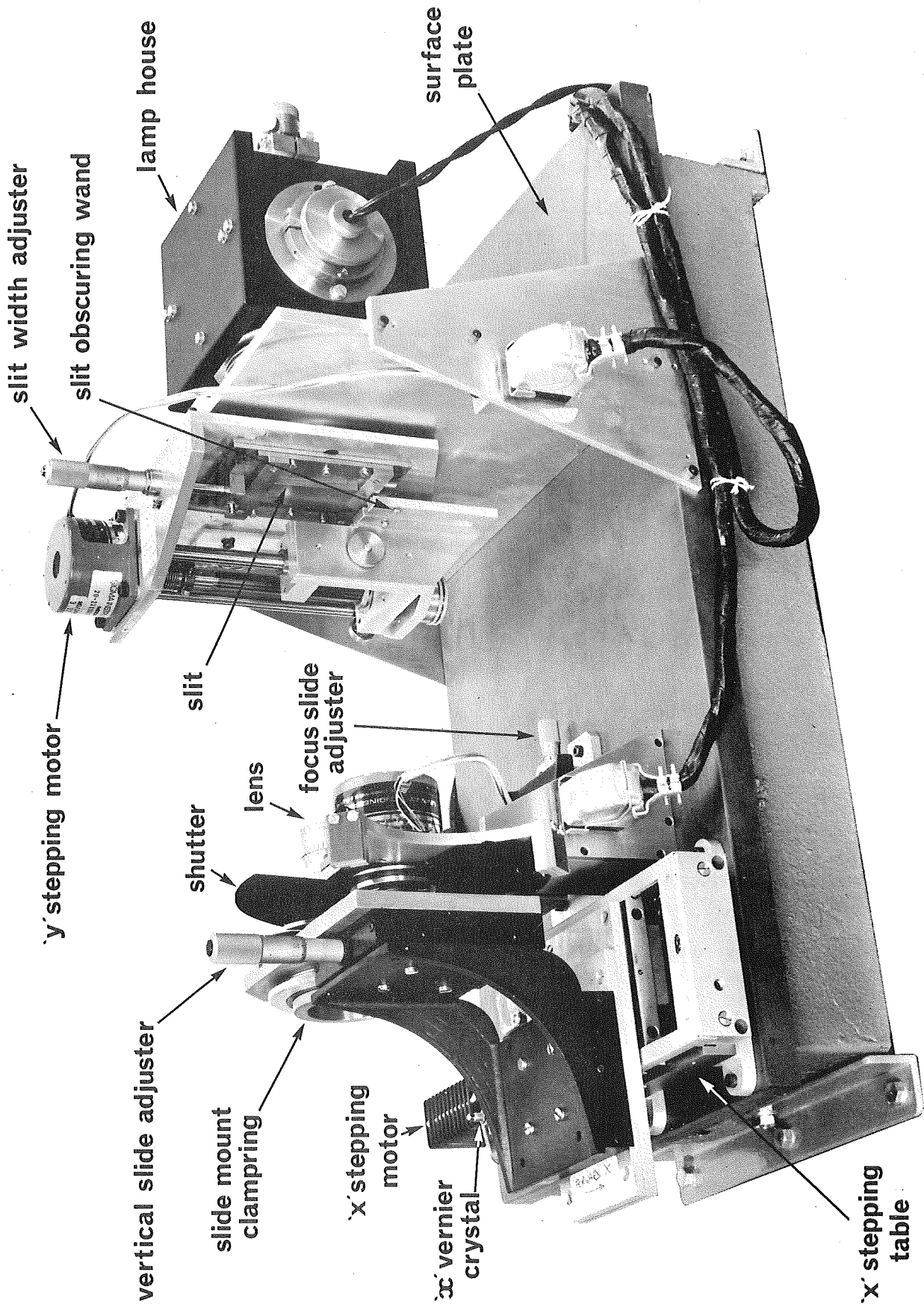


Fig. 4 - The stepping camera

2.1. Construction

2.1.1. Object slit and lamp-house assembly

The lamp house contains a 100 Watt, 12 Volt, class A1/45 quartz-iodine projector lamp, with a mirror and condenser lens assembly to illuminate evenly the 50 mm object slit. The lamp is powered from an adjustable stabilised supply, normally set to 11 Volts to extend lamp life and improve reliability. Connections to the lamp are soldered using a high melting point solder since a conventional socket can develop sufficient contact resistance to cause instability in the light intensity.

The object slit, projected on to the mask to form the image of one finger, is formed by a pair of machined metal jaws riding in a fork with a 10 : 1 slope, the fork position being set by a calibrated thimble; thus very fine control over slit width is attained. A stop was fitted to the mechanism to prevent complete closure of the slit, after some initial edge damage was noted due to the crushing of dust particles in the jaws. The minimum slit-width attainable at the time of writing was about 70 μm , representing a minimum finger width of about 8 μm on the slide.

The slit was widened at each end such that consecutive images, side by side on the slide, would be joined at each end by busbars, formed by overlapping these widened regions. Thus, each projected image comprised an electrode and its interconnections with the remainder of the device.

A carriage, mounted to one side of the slit, carries an obscuring wand 700 μm in diameter, arranged to obscure the slit to form the finger-break needed for transducer apodization. The carriage can be traversed over the entire length of the slit on a 1 mm pitch lead-screw in 5 μm increments, using the 'Y' stepping-motor, and is replacable by other carriages carrying wands or plates of any width and shape.

The complete assembly of the object slit, 'Y' stepping-motor and carriage can be rotated on its axis by $\pm 45^\circ$ and locked in position using a calibrated locking ring. The entire assembly of object slit, 'Y' motion and lamp house is rigidly mounted on a heavy surface plate.

2.1.2. Lens and shutter assembly

The lens is a 25 mm focal length, 16 mm cine lens and is mounted on a vertical bracket which is supported by a ball-slide mechanism

fixed to the surface plate. Precise positioning of the lens is obtained by a calibrated thimble operating on the ball-slide.

The shutter, a two-bladed opaque fan rotated by a stepping-motor, is similarly mounted on a bracket on the surface plate. Feedback to the control circuits from two opto-isolators indicates the open or closed state of the shutter.

2.1.3. Slide carrier and stepping table

The slide holder has three independent motions. The main, horizontal component is by means of a stepping-table, moved on a 1 mm pitch lead-screw in nominal 2 μm increments by the 'X' stepping-motor. Its total travel is 50 mm. The 2 μm increment can be bridged by the effect of a piezo-electric crystal translator expanding to move a horizontal slide which is mounted on the stepping-table.

Vertical adjustment of the slide holder is provided by another slide mounted on the stepping-table, with a calibrated adjusting thimble. The slide holder itself comprises a reference surface against which the photo-sensitive plate is clamped in its removable holder, by a screw-in clamp ring. The whole assembly can be rotated and clamped in any position over $\pm 45^\circ$. For initial focus adjustment, a microscope was mounted in a threaded block which could be inserted in place of the slide holder clamp ring.

2.2. Control

Manual and automatic control circuits were developed but neither will be dealt with here in great detail. All three motors are driven by commercial stepping-motor drive-cards, controlled by logic signals.

2.2.1. Manual controls

The 'X' and 'Y' motors can each be single-stepped or allowed to run at a preset speed in either direction. Two three-position switches (centre 'off'), connected to the motor cards via suitable logic, perform these functions. The first operation of a switch causes a single-step movement, 'fast' running occurs after about 0.5 s if the switch is still operated.

The shutter motor is not single-stepped but can be made to run at its preset speed in either direction by operation of a third switch. The shutter can be opened for a preset time by pressing a button which causes the motor to be driven

twice, separated by the time which is set by a further control. As described above, two optoisolators sense the position of the shutter. Exposure times of 1 to 10 seconds are available.

2.2.2. Automatic controls

A micro-computer system performs all the functions of the automatic control system. Data from a paper-tape reader is used to specify the positions of the 'X' and 'Y' travels and the vernier crystal. The computer controls the motor drive-cards to produce the desired movements, allows a short settling time, then opens and closes the shutter for a time preset on a pair of thumb-wheels. Exposure times can be set in 100 ms increments from about 1 s to 9.9 s. The vernier crystal setting is monitored on two hexadecimal displays on the control panel.

An automatic run of the machine can be started only if the shutter is closed and the tape reader is set to the correct mode. While an automatic run is in progress, all the manual controls and the tape reader controls are disabled to prevent accidental interference in the run. At the end of a run, and controlled by data from the paper-tape, the computer performs a self-checking routine and indicates the results of the check. A 'bad' indication implies that the control system has found errors in the paper-tape data.

An indication of the number of such errors is given in the vernier crystal monitor-displays.

2.3. Performance

Performance assessment falls into two categories, namely measurement of the accuracy and repeatability of the mechanical movements, and calibration of the controls in terms of the way in which focus and exposure affect reproduced lines (fingers of a transducer).

2.3.1. Mechanical movements

2.3.1.1. 'Y' motion

There is no evidence of any significant errors in the 'Y' motion such as non-linearity. Running at its high, synchronous, speed the stepping-motor can move the obscuring wand from end-to-end of the object slit in approximately 10 seconds. Wand movements are always made at this high speed because it is above a range of speeds at which the movement is unreliable due to the effects of inertia loading on the motor. There is no evidence of the motor de-synchronising as it accelerates or decelerates through such a speed range.

The obscuring wand has proved suitable in all experiments completed to date.

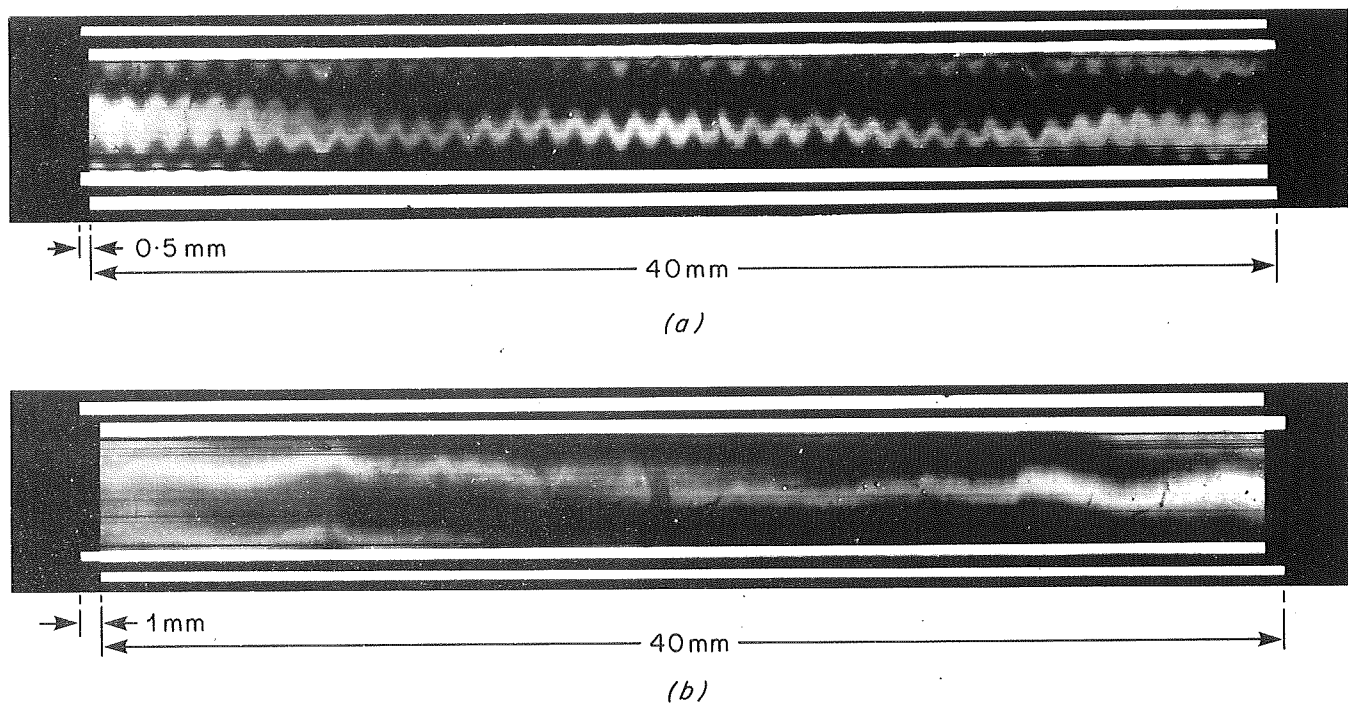


Fig. 5 - Moire' fringe interference patterns between $20 \mu\text{m}$ pitch transducers

(a) Maximum, showing enhancement of pitch variation

(b) Minimum, showing cancellation of pitch variation

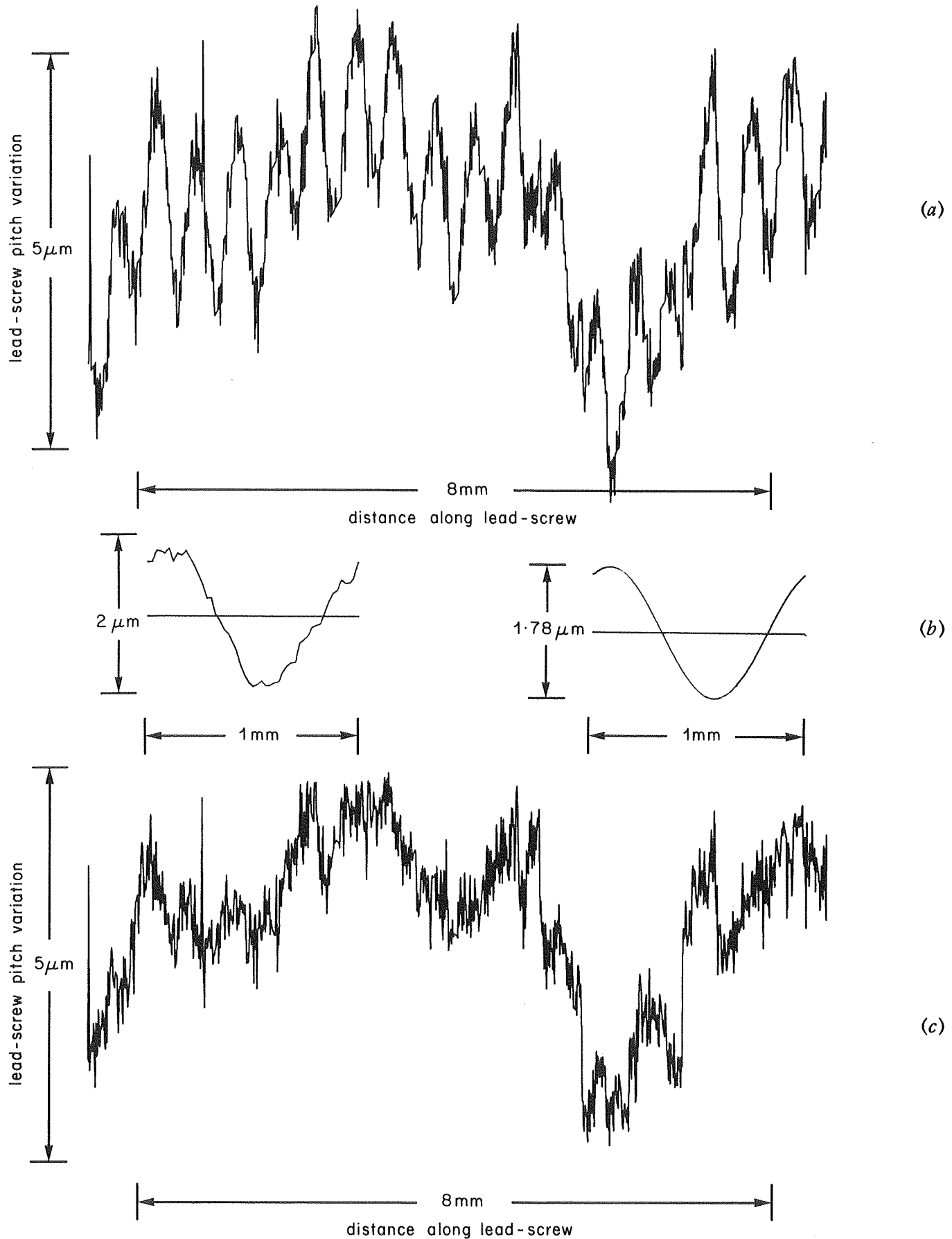


Fig. 6 - Computer-aided analysis of lead-screw pitch variation

(a) Plot of part of 2000 measurements

(b) Error cycle averaged over central region, and smooth curve used for correction

(c) Predicted pitch variation using correction

2.3.1.2. Shutter motion

The two bladed shutter can be made to rotate at about 1 revolution/second. Again, this is above a range of troublesome speeds, and it has proved satisfactory in use. Positioning of the opto-isolators placed a requirement on the shutter to come to rest in its closed position on only one of its 200 rest positions. However, this was not found to be a problem and the shutter operation has proved to be satisfactory.

2.3.1.3. 'X' motion

The accuracy of the 'X' motion over 40 mm of its travel is extremely good, backlash is approximately $3 \mu\text{m}$. Measurements of a mask exposed on the machine, containing 2000 fingers spaced at $20 \mu\text{m}$ intervals, revealed an accumulated deviation from the nominal value of only $23 \mu\text{m}$, representing 0.0575%. It is not known whether this difference is in the 'X' motion or in the travelling microscope used for the measurement. It is worth noting that an error of this magnitude when applied to a SAW device made on lithium niobate corresponds to an error such as would be caused by a temperature change of approximately 6C° .

Further measurements made on the mask described above revealed a cyclic error in true pitch, approximately sinusoidal with a 1 mm pitch and about $2 \mu\text{m}$ peak-to-peak amplitude. This effect is illustrated in Fig. 5(a), which is a photograph of the moire' fringe interference patterns produced by the superposition of two identical 2000-finger masks, offset by 0.5 mm. It can be seen that there are 40 cycles of pitch variation, with an amplitude of approximately one tenth of the spacing between fringes, and this spacing represents the $20 \mu\text{m}$ finger spacing. Fig. 5(b) shows the effect of sliding the two masks apart by a further 0.5 mm, resulting in cancellation. Thus, the cyclic pitch perturbation is seen to be regular.

Computer-aided analysis of the measured deviation from true position of each finger of the pattern, averaged over the 40 complete cycles, has revealed no evidence of a second harmonic (2 cycles/mm) component which could have been introduced by the 0.5 mm pitch lead-screw of the measurement microscope. Part of the 2000 measurements of the finger positions is shown graphically in Fig. 6(a). The average pitch error of a central group, the portion of the lead-screw most likely to be used, is shown in Fig. 6(b) and the result of subtracting this average from

the measurements over each millimetre is shown in Fig. 6(c). Allowing for measurement errors, the resulting deviation from true pitch is seen to be remarkably small. Accordingly, the average pitch error cycle was stored numerically in the control micro-computer programme in order substantially to correct the error using the piezo-electric translator. At the time of writing, however, this correction method had not been tested.

2.3.1.4. Vernier crystal motion

The piezo-electric translator is claimed by its makers to expand by approximately $10 \mu\text{m}$ on application of 1000 Volts. The crystal drive circuit comprises a 6-bit digital-to-analogue converter supplying voltages from 0 to +196 Volts, representing a translator motion range of 0 to $63/32 \mu\text{m}$. Such small movements are difficult to detect by direct means, but evidence accumulated from several attempts to use the crystal pointed to an instrumental fault. This problem is still being investigated.

2.3.2. Calibration

Many experiments have been performed to obtain accurate calibration of the control settings. After each improvement in the fabrication technology (see Section 3 below) most of these calibrations altered substantially. Thus it is meaningless to present complete calibration data for the machine, and only typical data will be given.

2.3.2.1. Focus

Many focus measurement experiments have been conducted, each taking the form of varying the focus setting, about a datum obtained using the focus microscope (mentioned in Section 2.1.3), between successive exposures on a single mask. The result of such an experiment is shown in Fig. 7. The focus setting for minimum finger width is not critical; an error of $\pm 24 \mu\text{m}$ in setting results in a width variation of only $0.5 \mu\text{m}$, implying a depth of field of about $40 \mu\text{m}$ with the lens working aperture of f/3.2. A measure of the variation of finger width across the travel of the stepping table is shown for a particular mask in Fig. 8. Evidently the true focus setting changes insignificantly. Changes in finger width are more affected by other factors, such as uneven resist-coating thickness. This result implies that at the time of making the mask described in Fig. 8, the 'X' motion was truly orthogonal to the optical axis of the lens.

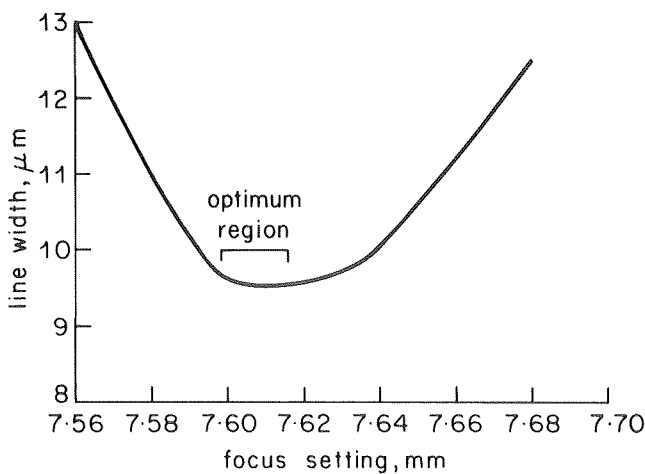


Fig. 7 - Variation of line width with focus setting

It is worth noting that masks made with an incorrect focus setting are often usable, the only visible effect for focus errors of up to $\pm 75 \mu\text{m}$ is that the fingers are broadened, but their edges remain sharp and straight.

2.3.2.2. Exposure

Correct exposure of photo-resists is important in projection systems such as the stepping camera, as over-exposure can cause fogging of the resist, in ideally unexposed areas, due to lens flare. Correct exposure is even more important with the particular negative-working resist used in these processes as it has non-linear properties, which are described in more detail in Section 3.2.4. The result of a typical exposure experiment is shown in Fig. 9, relating line width and exposure for a fixed width of the object slit. A suitable working exposure, taken at optimum focus, would be 2.5 seconds, where the rate of change of line width with exposure is low, but the resist is not saturated; an exposure variation of $\pm 10\%$ then causes a width variation

of less than $\pm 0.25 \mu\text{m}$.

The variation of line width with the voltage applied to the lamp is low, typically $1 \mu\text{m}$ Volt. However, considerable variations can be expected until the lamp and its power supply have stabilised. This takes, typically, 10 minutes from switching on.

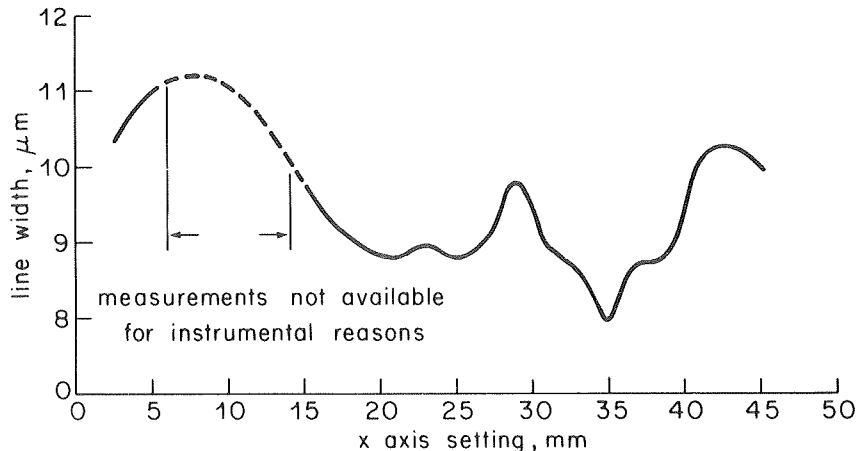
The experiment was carried out at several focus settings, and illustrates one of the non-linear properties of the resist. It can be seen in Fig. 9 that line width increases rapidly with exposure until saturation occurs, as at 3 seconds. Thereafter, increased exposure may cause a reduction in line width; it is supposed that this is caused by a local desensitisation of the resist resulting from the early part of the exposure. It should be noted, however, that this non-linearity is evident only when the resist is exposed in a projection system, and then is most marked when successive images are laid down side-by-side.

2.3.2.3. Line width

As described above, the line width is affected by both exposure and focus, but only to small extent; the main control of line width is determined by the object slit itself. A calibration chart relating line width with slit adjuster setting is given in Fig. 10. The line has a slope of $1/90$, being the product of the magnification ($1/9$) and the slope of the ramps holding the slit-forming jaws ($1/10$). It should be noted that a contact copy of a mask, using a positive-working resist, as in device fabrication (see Section 3), will have lines approximately $1 \mu\text{m}$ narrower than those in the mask.

Lines of $6 \mu\text{m}$ width have been produced, but these have irregular edges caused by inadequate lens resolution. Lines $8 \mu\text{m}$ wide can be

Fig. 8 - Variation of line width across the X axis of the camera at optimum focus



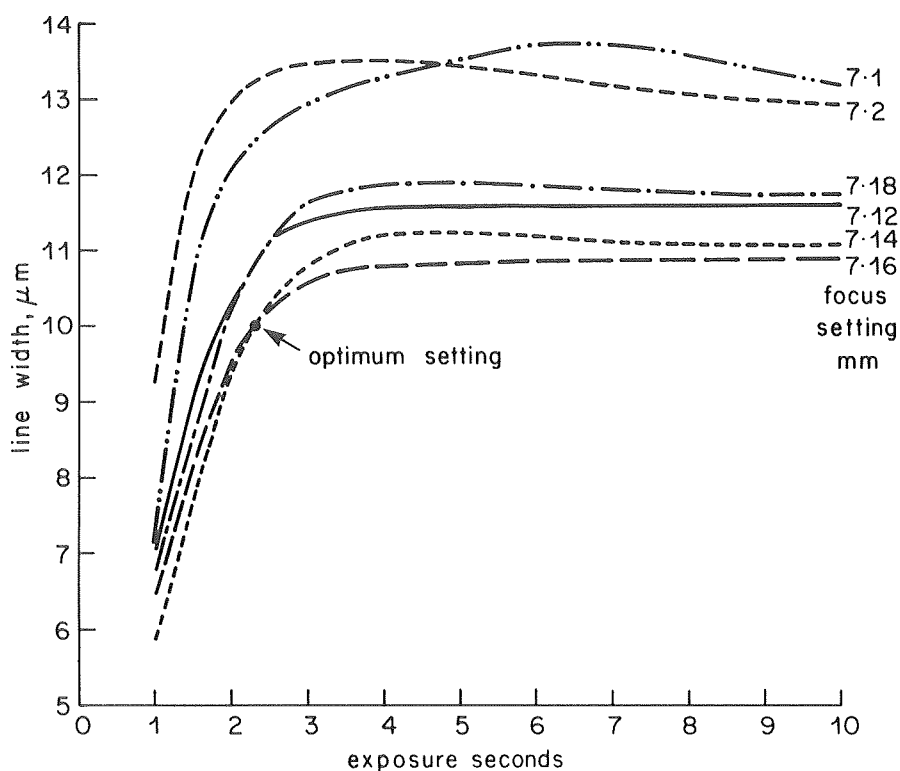


Fig. 9 - Variation of line width with exposure time at various focus settings

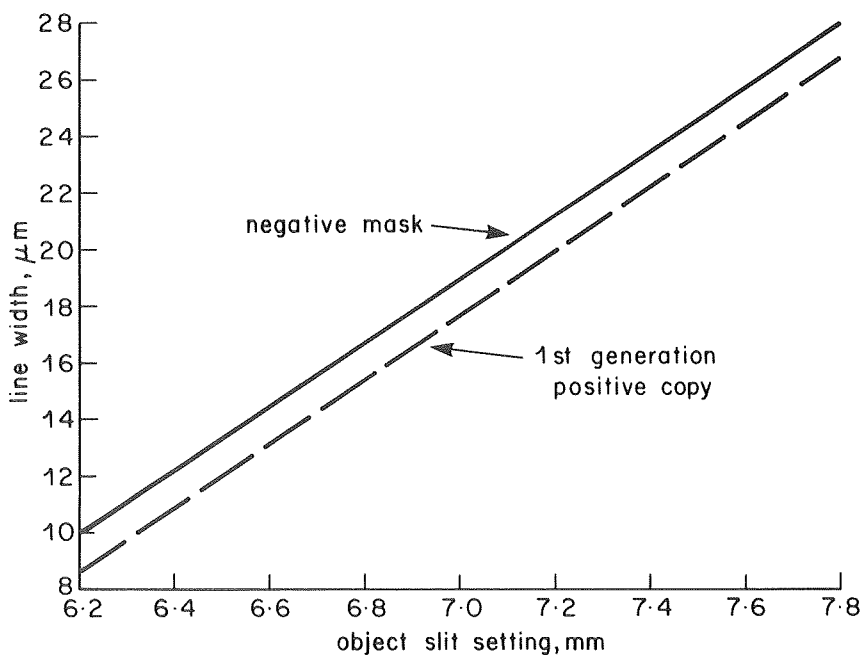


Fig. 10 - Variation of line width with object slit setting

produced reliably, suitable for SAW devices operating at 100 MHz, or low-loss devices on lithium niobate at 50 MHz when double fingers with half-width lines are required. It is reasonable to believe that the processes described in Section 3 could yield even narrower lines if a lens with better resolution were to be used.

3. Fabrication processes

3.1. Methods

The simplest method of making a SAW device using the camera described above would be by directly exposing a negative-working resist on a

metal-coated piezo-electric substrate in the camera, and etching the unwanted metal from around the developed image. However, it is much more convenient first to make a metal mask on glass having the required transducer patterns, and then to make the device itself or a number of identical devices using the mask as a template. This is the process used by commercial manufacturers.

It was decided at an early stage that final device production would use an ultra-violet sensitive positive-working resist* because of its high resolution capability and the ease of removal in safe solvents. Thus it was necessary to use a negative-working resist for making the mask directly in the camera. Several methods were tried before a successful technique was established.

Early experiments with an ultra-violet sensitive negative-working resist** were unsatisfactory but the cause was not found. Later experiments involved the fabrication of a positive mask using the positive-working resist and then making a negative copy of it. Contact printing on to a high-definition photographic plate promised success, but the line width attained was variable due to halation, and the final line width, produced by contact printing from it, was highly dependent on exposure.

A method of producing a negative mask by 'plating-up' was tried. This method first involved exposing and developing a positive image on to a metal film, electro-plating a different metal on to the metal film not covered by the exposed resist, removing the resist, and then etching away the original metal leaving a negative image in the plated metal. Several combinations were tried, plating copper or nickel on to bronze or on an aluminium/copper amalgam. Copper plating produced an image with fine filaments shorting fingers together. The etchant for bronze and aluminium/copper amalgam etched the nickel by vapour action and gave considerable undercutting, thus line widths were reduced by 4 or 5 μm .

Finally, a new ultra-violet sensitive negative-working resist*** was tried. This proved to be entirely suited to the requirements of our mask-making process, where the fact that the exposed resist is extremely difficult to remove is not important. It is believed that it could be removed

by immersion and agitation in hot dichlorobenzene, if needed for improved masks, but this has not yet been attempted due to the health hazards involved in using such a solvent.

3.2. Mask fabrication

The technique for mask production which has been developed and extensively tested is fairly straight-forward. The transducer pattern is produced in aluminium on a 50 mm square glass slide, using a negative-working photo-resist, details of the process and its development are given below.

3.2.1. Slide preparation

Slides are purchased ready polished and cleaned, it remains only to remove surface dust and the results of any accidental contamination. Washing in a detergent is sufficient but drying the slide then becomes difficult without leaving further contamination. The procedure finally adopted is to subject the slide to ultrasonic agitation in hot, filtered, de-ionised detergent solution, rinse in filtered water, then place in a vapour degreaser containing boiling isopropyl alcohol. On removal, surface moisture evaporates in seconds leaving the surface clean.

3.2.2. Metal coating

This is a well-known process, involving the evaporation of a quantity of metal on to the slide under vacuum. A simple vacuum plant is used to coat up to three slides in one batch; the slides are further cleaned by ion bombardment before evaporation.

Aluminium/bronze was originally used for mask production in order to facilitate subsequent plating, but with the advent of a reliable negative resist process, aluminium was used because of its good adhesion properties, especially to clean glass. Typical coating thicknesses are 50 to 200 nm. Thin layers are the least likely to suffer from etchant undercutting but they are the most prone to subsequent mechanical damage.

3.2.3. Resist coating

Photo-resist protects the thin metal coating as well as having its normal photographic function. Resist is applied from a medical syringe via a filter to remove solid contaminant particles, and a uniform resist coating is obtained by spinning the slide at a predetermined speed. Any solvents remaining are driven out by baking the slide, typically 20 minutes at 80°C. Using the negative

* Shipley AZ1350.

** Kodak Thin Film Resist.

*** Kodak micro resist 752.

resist diluted with an equal quantity of its thinner, a coating of thickness of 1 μm can be obtained reliably. However, using other dilutions and spinning speeds, thicknesses from 0.3 to 8 μm can be obtained. Ultrasonic agitation must be used to ensure complete mixing of the resist and thinner. Experiment has shown that 1 μm represents a good compromise between resolution and metal protection.

3.2.4. Exposing the resist

First experiments with exposure of the resist gave conflicting and confusing results. Eventually, these were attributed to a general non-linearity in its performance. This takes the form of a reduction of reproduced line-width with increased exposure above normal saturation, as described in Section 2.3.2.2 and illustrated in Fig. 9. Confirmation of this effect was obtained by further experiments in which lines of constant width were exposed at ever decreasing spacings. Over-exposure of the widened ends, forming the connecting busbars, caused a local desensitisation of the resist resulting in lines not joining the busbars. This effect became more evident where the lines should have overlapped each other, except in the gap caused by the obscuring wand. Instead, the lines contracted except where adjacent to such a gap and this situation is illustrated in Fig. 11.

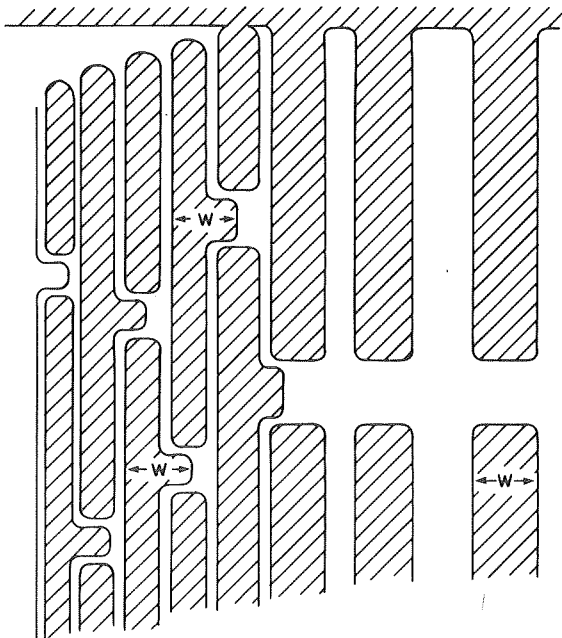


Fig. 11 - The effect of resist non-linearity on lines of constant width W exposed one at a time from right to left, and with progressively reduced spacing

Adoption of a lower exposure, as described in Section 2.3.2.2, reduced these effects to an acceptable level. It is important, in each exposure, to ensure that there is only minimal overlap of the busbar regions of the lines, since the connecting busbars are formed by overlapping exposures of the widened ends of the slit image.

3.2.5. Image development

Using proprietary chemicals, the image can be developed either by spray or by immersion and both have been investigated. Spray development is rapid, typically 30 seconds, whilst dish development can take up to 2 minutes. Spray development is the more reliable, but the health hazards from spraying the toxic, flammable, chemicals are considerable and therefore most attention was given to establishing a reliable immersion process. Considerable agitation is essential throughout the process to avoid local exhaustion of the developer.

After development, the slide is washed in a proprietary rinse. Again, spraying is faster and better than immersion and constant agitation is essential in the immersion process. After rinsing, the image is dried and this can best be accomplished by high-speed spinning.

It should be noted that all the chemicals used in these processes are volatile toxic irritants and have low flash-point temperatures. They are dangerous and must be handled with care in a well-ventilated environment.

3.2.6. Etching

The mask is formed by etching away the metal layer, using the resist image as a template. The negative resist is highly resistant to solvents after exposure and almost any acid etchant can be used. For the early experiments using aluminium/bronze coating, a mixture of hydrochloric acid and ferric chloride was used as an etchant giving etching times of 3 to 5 seconds. The change to aluminium coating brought a need for a new etchant. A mixture of nitric acid, acetic acid and phosphoric acid,* all in concentrated form was found to be suitable. Etching times depend on metal thickness but 2 minutes at room temperature is typical. The can be reduced considerably at a higher temperature; for instance it is only 30 seconds at 45 °C.

* This etchant is commonly used by commercial and experimental SAW device manufacturers.

The mixture is highly viscous and bubble formation while etching can result in poor images. The mix is allowed to outgas before etching during which some gentle agitation is needed.

When etching is complete, the slide is washed and dried by a short high-speed spin.

3.3. Fabrication of a device from a mask

This Section summarises the processes involved in making a device from a mask. Care and cleanliness are still important in these final stages.

3.3.1. Substrate mounting

Device substrates are small and often delicate and are best handled mounted on a glass slide. Any non-permanent adhesive can be used; thermoplastic optical cements are particularly suitable. The glass slide is built up around the device with glass pieces, so that the device substrate is slightly proud of its surroundings.

3.3.2. Cleaning

Traces of the adhesive are removed from the polished surface of the device substrate by repeated washing in a solvent such as trichloroethylene. The cleaning process then follows that described in Section 3.2.1.

3.3.3. Metal coating

The process described in Section 3.2.2. can be used, and both substrates and slides can be coated together. Aluminium coatings are normally used.

3.3.4. Resist coating

Positive-working resist is used because of its ease of removal after use, in a safe solvent such as acetone. The resist is applied, undiluted, from a medical syringe through a filter to remove solid particles. A uniform coating is obtained by spinning the slide at a pre-determined speed. Subsequent baking is used to drive out residual solvents. Typically, spinning at 1000 r.p.m. for 1 minute and baking at 60°C for 10 minutes gives a coating thickness of 0.75 µm, which has proved to be satisfactory. Other thicknesses can be obtained by dilution and variations in spinning speed and duration. Excessive baking merely reduces the photo-sensitivity of the resist.

3.3.5. Exposure and development

The resist-coated substrate and the slide carrying the metal mask are held together, resist-coating to metal, in a vacuum clamp. This ensures intimate contact. The resist is exposed, through the mask, in an ultra-violet light box; the exposure duration is typically 45 seconds. Exposure is not critical, as it is not possible to over-expose a positive-working resist.

Using a commercial, mildly alkaline, chemical developer the image is fully developed in 30 to 45 seconds. Shorter development times are possible, but the longer times ensure removal of any thick bead of exposed resist around the edge of the substrate.

The developer is washed off in running water, and a short spin at high speed dries the image.

3.3.6. Etching

The procedure described for aluminium in Section 3.2.6 is used.

3.3.7. Mounting the device

The device is removed from its glass mount and rigidly fixed to a suitable electrical mount, again using an adhesive such as optical cement. The electrical connections are made using fine wires attached by electrically conductive paint or by thermo-ultrasonic bonding to the device busbars.

4. Conclusions

A stepping camera has been constructed, and photo-chemical processes have been developed for the fabrication of SAW devices. Although not described in this Report, a number of experimental devices have been made during the development of the processes. At the time of writing, the yield was fairly low, typically 25% overall. This could probably be improved by scrupulous attention to cleanliness.

Further work on the vernier crystal will be needed when it is refitted to the camera, and an assessment of the 'X' motion pitch-error correction can then follow.

Although the original aim of this work has not yet been fully achieved, it is within sight, and a safe and mostly reliable facility for produc-

ing experimental SAW devices without the need for conventional artwork has been established. Experimental assessment of the performance of SAW devices made with this facility will be the subject of future Reports.

5. References

1. LORD RAYLEIGH. 1885. On waves propagated along the plane surface of an elastic solid. *Proceedings of London Mathematical Society*, 1885, **Vol. 17**, pp. 4 – 11.
2. WHITE, R.M. and VOLTMER, F.W. 1965. Direct piezo-electric coupling to surface elastic waves. *Applied Physics Letters*, 1965, **Vol. 7**, pp. 314 – 316.
3. SLOBODNIK, A.J. Jr., DELMONICO, R.T., CONWAY, E.D. 1973. *Microwave Acoustics Handbook*, Vol. 1A. 1974. *Micro-wave Acoustics Handbook*, Vol. 2. Massachusetts, Air Force Cambridge Research Laboratories, Air Force Systems Command, USAF.
4. SMITH, W.R. and PEDLER, W.F. 1975. Fundamental- and harmonic-frequency circuit-model analysis of interdigital transducers with arbitrary metallisation ratios and polarity sequences. *IEEE Transactions on Microwaves*, **Vol. MTT-23**, No. 11, November 1975.
5. MASON, W.P. 1948. *Electromechanical transducers and wave filters*. 2nd edition, Princeton N.J., Van Nostrand, 1948, pp.201 – 209, 399 – 409.
6. HAYS, R.H. and HARTMANN, C.S. 1976. Surface-Acoustic-Wave devices for communications. *Proceedings of IEEE*, **Vol. 64**, No. 5, pp. 652 – 670, May 1976.
7. MAINES, J.D. and PAIGE, E.S. 1976. Surface-Acoustic-Wave devices for signal processing applications. *Proceedings of IEEE*, **Vol. 64**, No. 5, pp. 639 – 652, May 1976.
8. MURRAY, R.J. and READ, E. 1977. Surface-Acoustic-Wave transversal bandpass filters. *General Electric Company Journal of Science and Technology*, **Vol. 44**, No. 1, 1977.
9. SKEIE, H. and ENGAN, H. 1975. Second-order effects in acoustic surface-wave filters: design methods. *Radio and Electronic Engineer*, **Vol. 45**, No. 5, pp. 207 – 220, May 1975.
10. WAGERS, R.S. 1976. Spurious acoustic responses in SAW devices. *Proceedings of the IEEE*, **Vol. 64**, No. 5, pp. 699 – 702, May 1976.
11. MATTHEWS, H. 1977. *Surface wave filters, design construction and use*. J. Wiley and Sons, New York, 1977.
12. RICH, G.J. 1976. Pattern generation and replication for SAW devices. *Wave Electronics*, **Vol. 2**, Nos. 1, 2, 3, pp. 219 – 237, July 1976.